Rev.Adv.Mater.Sci. 7 (2004) 67-74

DEFORMATION MECHANISMS IN A NANOCRYSTALLINE VITROPERM ALLOY

A.V. Sergueeva, N.A. Mara and A.K. Mukherjee

Chemical Engineering & Materials Science, University of California, One Shields Avenue, Davis, CA 95616, USA

Received: July 29, 2004

Abstract. In the current investigation, microstructures with different grain sizes in the nanorange were obtained in an initially amorphous Fe-based alloy by controlling annealing parameters. The as-annealed samples revealed microstructures of varying morphology, and these different states were tested in tension in a wide range of temperatures and strain rates. The microstuctural information and the mechanical data obtained from these tests were analyzed in the context of plasticity at diminished length scales. Special emphasis is given to the difficulty of intragranular dislocation generation inside the matrix in truly nanoscale structures and its implication to affect slip accommodation processes in current models of nanocrystalline plasticity at elevated temperatures.

1. INTRODUCTION

In general, in order to understand the nature and origin of deformation mechanisms at high temperatures, information related to the dependence of strain rate on stress, temperature, and grain size is essential. In the case of nanocrystalline materials (NCM), one way to obtain this type of information is adopting an effective method that would produce NCM with different grain sizes and then performing systematic tests under identical conditions of temperature and stress for the purpose of determining the values of the grain size sensitivity.

Despite recent efforts devoted to studying the elevated temperature behavior of NCM, data obtained by different investigators are either not consistent in trend or too limited in scope. Based on findings in the literature, the characteristic strain rate exponent values encountered during high-temperature deformation of nanometals can range widely, as can the activation energy for deformation. These values will usually vary from lattice diffusion to grain boundary diffusion of certain species responsible for controlling the rate of deformation, depending on the deformation mechanism at hand [1-5]. There are two possible reasons for such variations. First, mechanical properties in NCM are very sensitive to their initial microstructures. This sensitivity is the result of the non-equilibrium nature of NCM. Because of this characteristic, two grades of a nanocrystalline material (same composition and structure) that are prepared by different procedures and that have a similar grain size may exhibit different mechanical properties. On this basis, discrepancies may exist when comparing experimental data reported by investigators who used different processing techniques in producing material with the same nanocrystalline grain size. Second, it is very difficult to produce bulk NCM free from porosity and other flaws and having a wide range of grain size. Because of this difficulty, the dependence of strain rate on stress, grain size, and temperature in NCM is, at present, unclear.

To best fill in some of these knowledge gaps, what is ideally needed is a specimen that has uniform chemistry, that is relatively stable at high test temperatures, and where a method for varying the grain size from a few nanometers to a few microns would be available. Production of fully dense,

Corresponding author: A.K. Mukherjee,e-mail: akmukherjee@ucdavis.edu

nanocrystalline samples with a microstructure that has both a relatively large number of slip systems and is stable at test temperature is paramount to the investigation of the role of interface sliding in nanomaterials. Furthermore, the production of microstructures with grain sizes smaller than ~30 nm can facilitate the experimental study of boundary sliding at increasingly smaller length scales, where previous investigation have been limited to computer simulations.

In this work, crystallization of an initially amorphous metallic glass is used as a method of obtaining a porosity- and contamination-free nanocrystalline material. A commercially available Fe-based metallic glass of the FINEMET type (Vitroperm) was chosen because it crystallizes into a single phase structure of α-Fe, which is stable at temperatures up to 600 °C. Samples with different grain size distribution within nanometer range (15-400 nm) were tested at different temperatures and strain rates. Results were analyzed in terms of a rate equation describing deformation behavior with respect to deformation parameters and microstructural evolution.

2. EXPERIMENTAL PROCEDURE

Strips of melt-spun Vitroperm ($Fe_{73.5}Cu_1Nb_3Si_{15.5}B_7$) metallic glass ribbon approximately 2 mm wide, ~20 microns thick, and with a gage length of 4 mm were used in this investigation. Tensile testing was carried out at a variety of strain rates using a custom-built mini tensile tester with displacement resolution of 5 microns and load resolution of ~1 gram that is capable of testing materials with a gage length and width as small as 1 mm, and thicknesses down to 5 microns. All testing was carried out in a high-purity (99.999%) argon atmosphere to minimize effects of oxidation. Annealing treatment was performed *in-situ* in the tensile tester prior to testing.

Microstructural analysis was conducted using a Philips CM-200 at 200 kV for all microscopy including EDS, EELS and high-resolution microscopy. X-ray analysis was performed using a Scintag XDS 2000 X-ray diffractometer with a 3 axis goniometer and Cu K_α radiation.

3. RESULTS

Three types of annealing were applied in order to crystallize the material. Bright field images of the alloy microstructure after various methods of annealing are presented in Fig. 1. Heat treatment at a temperature of 600 °C for 1 h provides optimal condi-

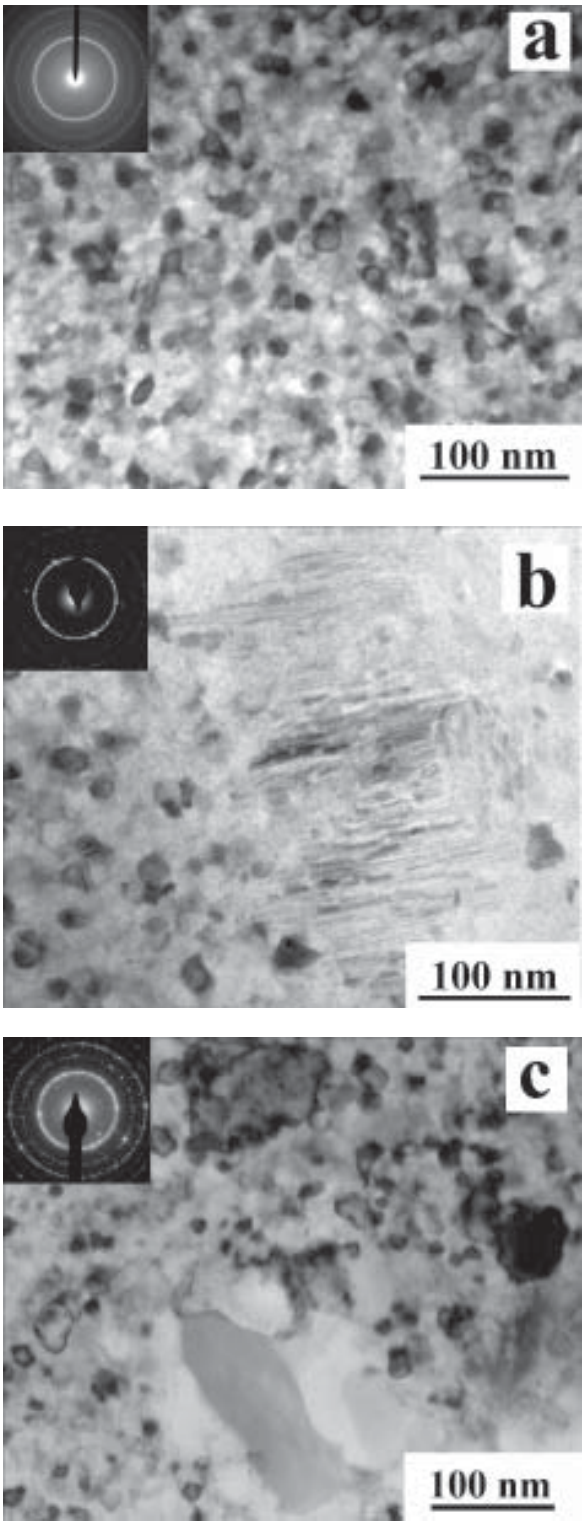

Fig. 1. Bright field image and selected area diffraction pattern of Vitroperm after annealing at (a) 600 °C for 1 h; (b) 600 °C for 5 h; (c) 650 °C for 1h.

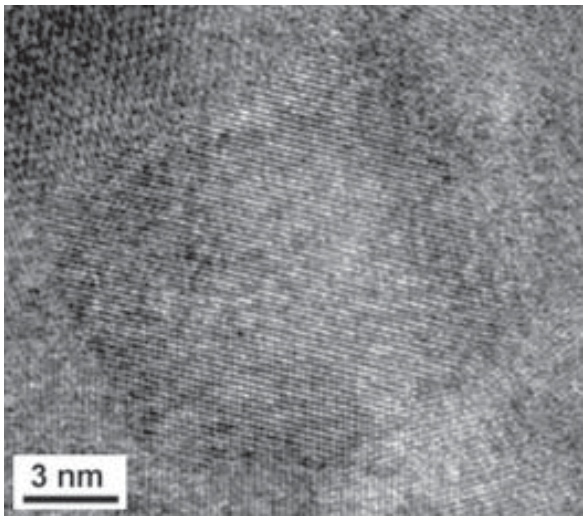

Fig. 2. HRTEM micrograph of Vitroperm after annealing at 600 °C for 1 hour.

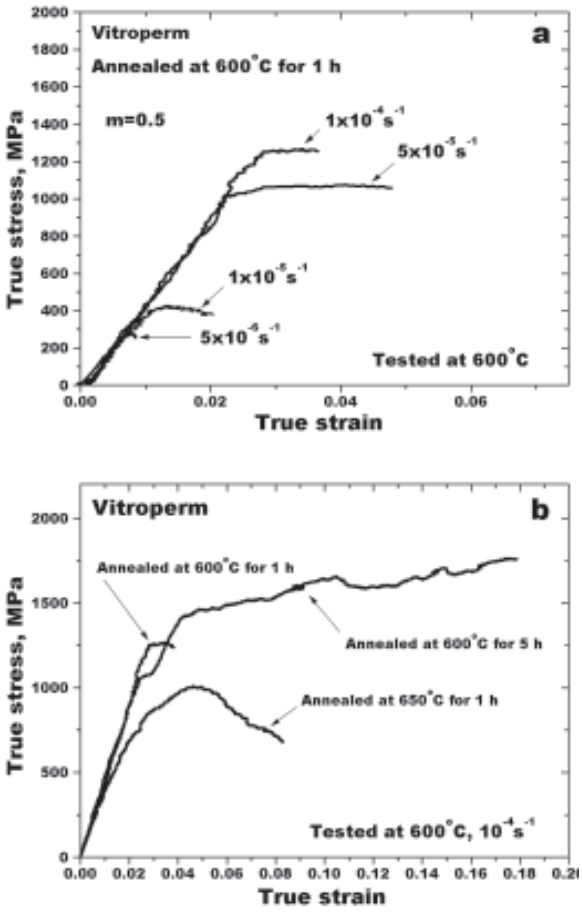

Fig. 3. True stress/True strain curve for Vitroperm tested at 600 °C: (a) after annealing at 600 °C for 1h and tested at different strain rates; (b) after different type of anealing and tested at 10^{-4} s^{-1}.

tions for creation of a homogeneous one-phase microstructure with extremely fine grains. (Fig.1a). In order to verify the absence of the residual amorphous phase at the grain boundaries, HRTEM investigation was carried out. Fig. 2 depicts a typical micrograph in which all of the boundaries and triple points investigated showed no evidence of a residual amorphous phase and appeared clean of contamination by other phases. Mean grain size is about 15 nm. The inset SAED patterns (Fig. 3a) confirm the formation of a single α-Fe phase. Increasing annealing time to 5 h leads to formation of a structure with a bimodal grain size distribution where distinctly separate large grains of about 200 nm with lamellar type morphology are randomly distributed in a matrix with mean grain size of about 15-20 nm (Fig. 1b). According to SAED pattern, these grains seem to have a plane spacing that closely corresponds to α-Fe, and similar peaks have been found in X-ray diffraction (XRD) analysis (not shown). However, local chemical analysis is intended to be carried out in the future to further confirm the composition of these areas.

Annealing at 650 °C for 1 h also results in formation of a structure with bimodal grain size distribution (Fig. 1c). But in this case, the large grains (100-200 nm) mostly arrange in groups that are randomly distributed in the α-Fe matrix with grain size of 15 nm and smaller. The presence of an additional phase (or phases) is evident from the SAED pattern.

Fig. 3a presents true stress-true strain curves for the alloy with the initially homogeneous single-phase nanocrystalline structure shown in Fig. 1a. When tested at 600 °C at varying strain rates, the material shows limited ductility of just a few percent but with a very high strain rate sensitivity value (m=0.5). This high m-value usually corresponds to a grain boundary sliding related elevated temperature deformation mechanism like superplasticity. Fig. 3b exhibits the mechanical response of all three types of annealed structure (shown in Fig. 1) at the same testing conditions (600 °C and strain rate of 10^{-4} s^{-1}). A strong dependence of mechanical behavior on structure is evident. Under the above conditions, the nanocrystalline material with homogeneous structure (Fig. 1a) has demonstrated elastic perfectly plastic behavior. Limited strain hardening was revealed after yielding at 1270 MPa. The formation of separate large striated or lamellar type grains in a nanocrystalline matrix (Fig. 1b) leads to an increase both in strength and plasticity. In this

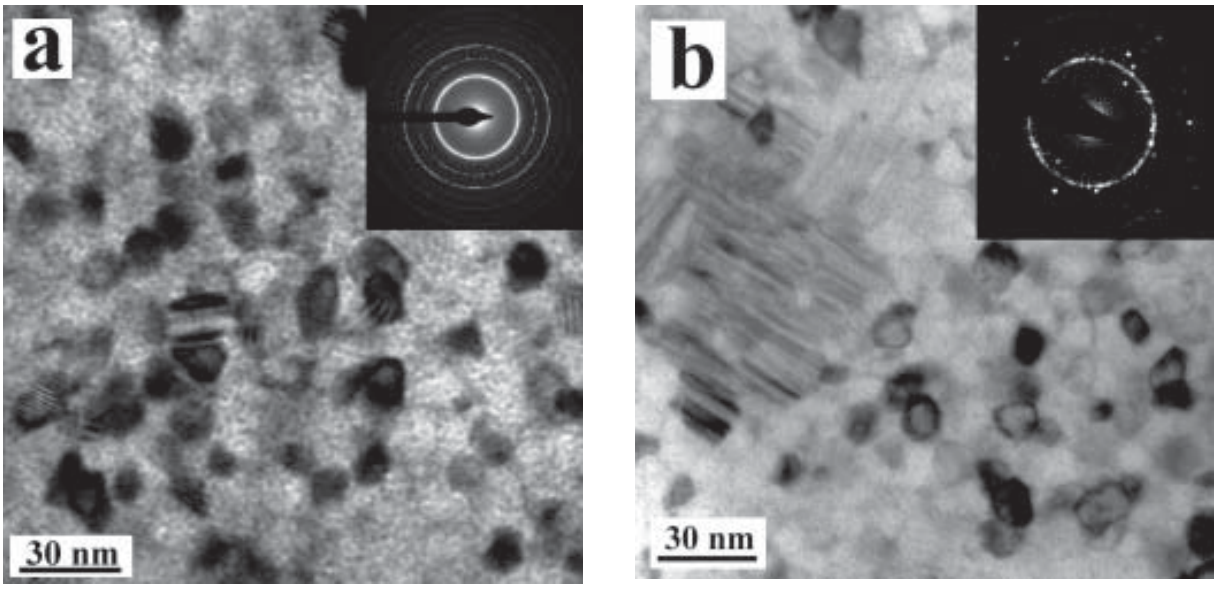

Fig. 4. Bright field image and selected area diffraction pattern of the samples tested at 600 °C and at strain rate of 10^{-4} s^{-1}: (a) initially annealed at 600 °C for 1 h; (b) initially annealed at 600 °C for 5 h.

case, despite unstable flow, the material exhibited an elongation of about 15% with well-pronounced strain hardening. The structure obtained after annealing at 650 °C for 1 h (Fig.1c) yields at a much lower stress of about 400 MPa, exhibiting extensive strain hardening and necking. Fracture stress is much lower than that for the other two structures, and uniform elongation is only about 3%.

A specific feature of the tested structures is their thermal stability at testing temperature. The initially uniform nanocrystalline structure (Fig. 1a) demonstrated no visible grain growth during testing at 600 °C, and retained the original one-phase microstructure (Fig. 4a). The bimodal structure (Fig. 1b) after 600 °C testing revealed two distinct microstructural features, with the retention of the lamellar grains in the fine-grained matrix of the initial structure (Fig. 4b). However, an additional feature is the precipitation of a new phase in the form of large isolated grains in a nano-matrix (Fig. 5). The size of the lamellar grains and their distribution remains similar to that in the initial as-annealed state.

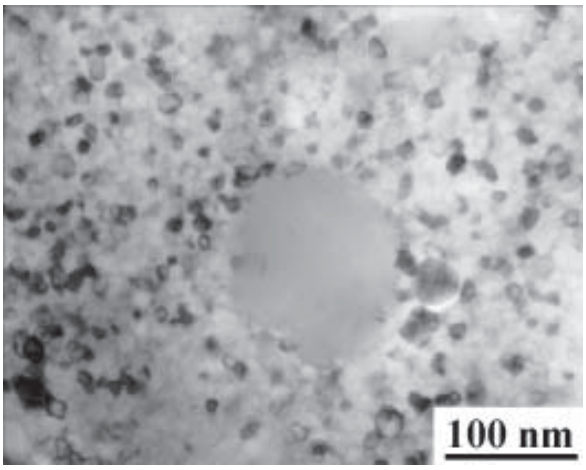

Fig. 5. Bright field image of the additional area in the sample gage shown in Fig. 4b.

At higher temperatures, the behavior of the fully nanocrystalline Vitroperm alloy with homogeneous structure is much different. Plasticity is enhanced, steady-state flow is reached, and flow stress values are much lower as seen, for example, for the sample tested at 725 °C (Fig.6a, curve1). As would be expected, the microstructure at the end of this test differs greatly from that found in samples tested at 600 °C, as is shown in Fig. 6b. From the selected area electron diffraction pattern and corresponding bright and dark field images, it is clear that a second phase has nucleated at some of the triple points, and the larger grains have grown to ~125 nm in diameter. However, the grains have remained remarkably equiaxed, considering that they have undergone 65% elongation. The alloy with bimodal grain size distribution (Fig. 1b) has shown

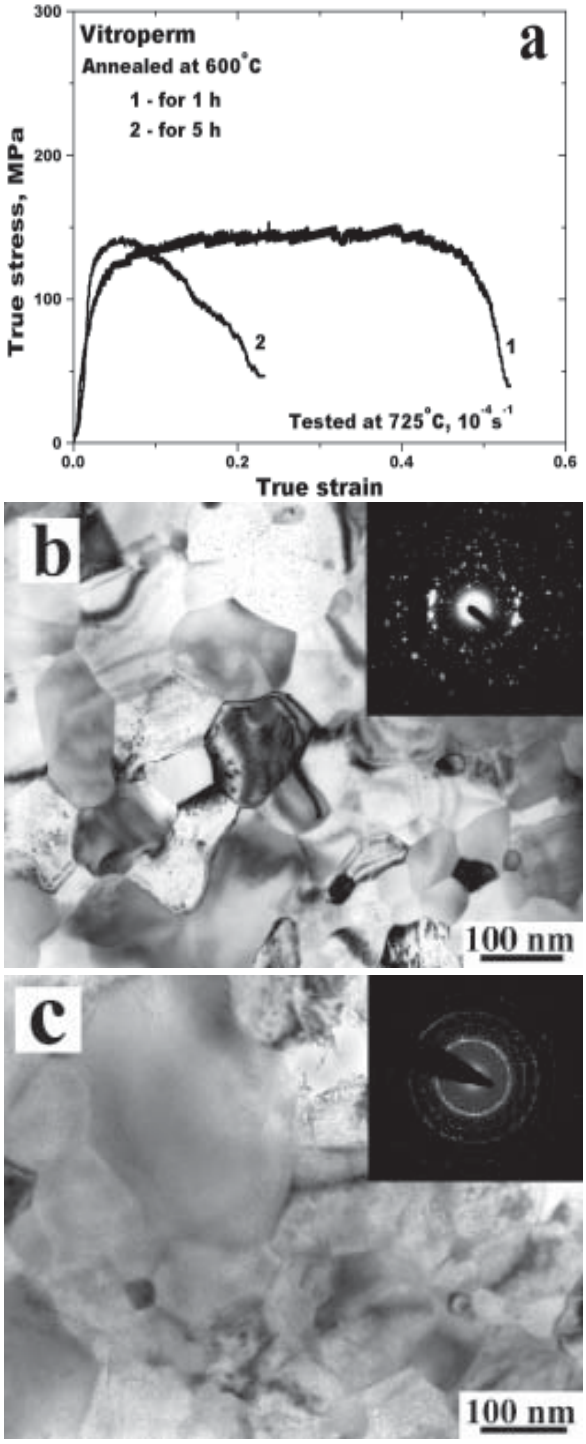

Fig. 6. (a) True Stress/True Strain for Vitroperm after 600 °C anneal for different time, tested at 725 °C; (b) and (c) bright field images and selected area diffraction patterns of the gage microstructure after deformation that correspond to curves 1 and 2, respectively.

slightly higher yielding and flow stresses but the material did not show much plasticity (Fig. 6a, curve 2) and extensive necking was observed. Upon evaluation of the post-tested structure (Fig. 6c), a multiphase microstructure with larger grains than those found in the previous 725 °C test are evident, along with dislocation activity in many of the larger grains.

Through the use of multiple tests at different temperatures and strain rates including several isotemperature strain-rate jump tests of the alloy after annealing at 600 °C for 1 h with mean grain size of 15 nm (Fig. 1a), a logarithmic true stress vs. logarithmic true strain plot can be constructed as depicted in Fig. 7. As is evident in the figure, there is a definite change in mechanism from the tests at 600 °C and those at 675 °C and above. The slope that gives m=0.5 points to grain boundary sliding as a deformation mechanism, which is usually associated with superplasticity, but in these tests at 600 °C, the deformation behavior is mostly elastic, with minimal plasticity (Fig. 3a). For the ductile specimens above 675 °C, the slope yields a strain rate exponent of 0.2 that is usually associated with power-law creep; a mechanism which depends on dislocation climb and lattice diffusion to accommodate the plastic flow, and may result in elongation of the deformed grains in the absence of grain rotation. We do not see elongation of grains that could correspond, for example, to 65% ductility in the post-tested TEM micrographs (Fig. 6b).

Crucial to the investigation of the rate-controlling deformation mechanism at temperatures of 675 °C and above is the composition of the grains in the sample after deformation. Electron Energy Loss Spectroscopy (EELS) and Energy Dispersive Spectroscopy (EDS) were carried out in an effort to find the components of the final microstructure. Most

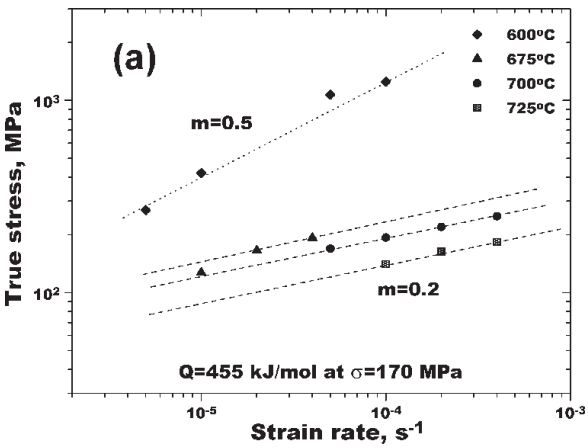

Fig. 7. Summary on stress-strain rate dependence for the alloy with initial mean grain size of 15 nm.

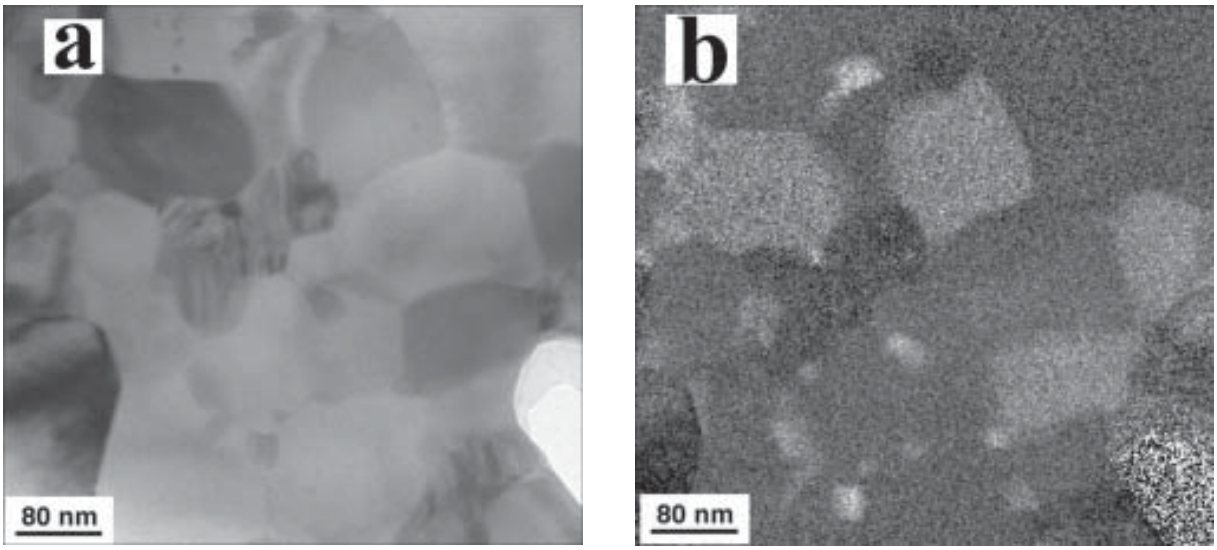

Fig. 8. (a) Bright field image of the microstructure after testing at 725 °C (same shown in Fig. 6b); (b) the EELS map of Nb, with the lighter areas corresponding to greater Nb concentration for the same area.

interestingly, an EELS map based on Niobium shows the segregation of Nb to some of the large grains, with the greatest concentration in the small particles at the triple points in Fig. 8. Further investigation using EDS confirms the EELS results, as well as reveals segregation of copper to the grain boundaries (not shown).

4. DISCUSSION

The three different types of initial nanostructures obtained in Vitroperm alloy by controlled crystallization give the opportunity of estimating the effects of microstructural parameters on deformation processes at diminished length scales. After annealing at 600 °C for 1 h, a homogeneous single-phase nanocrystalline structure with mean grain size of 15 nm was formed. High temperature mechanical property investigations for such grain sizes has to date been limited to computer simulations, making these tests the first experimental results under such conditions. This structure has demonstrated unique deformation behavior with a high strain rate sensitivity value corresponding to that of superplastic flow but with very limited ductility (Fig. 3a). Usually, for mechanisms with m=0.5, grain boundary sliding occurs, and at stress concentrations such as triple points, dislocations are emitted and slip and climb their way to the recovery site at another grain boundary to accommodate the deformation. This model assumes that the grain size is sufficient to permit dislocations to form and propagate through the grain interior or along grain boundaries. At grain sizes as low as 15 nm, it is intrinsically difficult to keep dislocations inside tiny nanocrystalline grains due to image forces and interactions with grain boundaries [6]. Actually, the material showed a behavior close to elastic perfectly plastic with almost no strain hardening (Fig. 3a). Similar lack of strain hardening was observed in other NCM and has been taken to imply the absence of dislocation activities or a fundamental change in deformation mechanism [7]. Moreover, the fraction of atoms in the grain boundaries is significant (about 15% at 15 nm, as estimated in computer simulations) and GB processes are expected to become increasingly important with decreasing grain size. High strain rate sensitivity observed in this material suggests active grain boundary sliding during deformation. However, in the absence of dislocations, there is no way to accommodate the strain after sliding has occurred, unless by diffusion-based mechanisms, which are probably not working fast enough in this case (at 600 °C) to avoid fracture. This results in a stress concentration at triple points that cannot be relieved, so a void nucleates and quickly grows, leading to early fracture. The strain rate exponent of m=0.5 corresponds to the actual sliding of the grains as the rate-limiting step for deformation, since no other

mechanism, especially those operated by dislocations, is present.

An increase in ductility was observed in this material in the case of the presence of large lamellar grains in a nanocrystalline matrix (Fig. 3b). Not only size, but also the distribution of these large grains seems to strongly affect the mechanical response of the material. The most attractive combination of properties (high strength and high ductility) was observed when the large grains were isolated in the nanocrystalline matrix (Fig. 1b). This structure displayed strength in excess of 1.5 GPa with adequate plasticity of 15% (Fig. 3b). It seems that dislocation activity in the large grains is responsible for strain accommodation in the nanocrystalline matrix and for enhanced ductility of the material, while the nanocrystalline matrix itself is responsible for the measured high strength. If the large grains are arranged in groups separated by the nanocrystalline matrix (Fig. 3c), the strength drops dramatically, and the material fails to show uniform plasticity (Fig. 3b). These groups of large grains most likely deform by dislocation creep at lower stresses. Actually, such coarse-grained groups seem to be formed during deformation of the initially uniform nanostructure at elevated temperatures and might be responsible for the transition in deformation mechanism between 600 °C and 675 °C (Fig. 7).

A strong effect of initial microstructure on mechanical response of the alloy was detected at higher temperatures as well. For example, at 725 °C, the initially homogeneous structure (Fig. 1a) has displayed steady state flow at relatively low stresses, while intensive necking was detected in the structure with initially bimodal grain size distribution (Fig. 1b). An uniform multi-phase structure with grain size of 70-150 nm was observed by TEM in the gage of the deformed samples with initially uniform structure (Fig. 6b). The presence of uniform structure seems to be crucial for support of steady state flow. Deformation of the initially bimodal structure with isolated large grains (Fig. 1b) results in formation of non-uniform structure with a wide grain size distribution from 20 to 400 nm (Fig. 6c), leading to extensive localized deformation and necking.

Moreover, for the tests at temperatures higher than 600 °C, there is evolution of another phase at the triple points of the original grains. The EELS results from Fig. 8 revealed the formation of Nb-rich grains at triple points throughout the structure. Other authors have found that in FINEMET metallic glasses, Nb tends to reside at the grain boundaries in the as-crystallized structure and will pin the boundaries, leading to a structure that is quite stable at high temperatures [8]. This coincides with the above results, in that the grain size is very stable up to a certain point, and once Nb is segregated to its own phase away from the α-Fe grain boundaries, grain growth of all phases quickly proceeds. Furthermore, if the 15 nm grains are too small to have dislocation activity to accommodate the deformation at triple points, it is logical that once the grains have grown sufficiently to allow dislocation motion that the strength should drop, and plasticity should increase. This is in fact exactly the trend that is exhibited in the data.

If clean, deformation-free grains are formed at stress concentrations such as triple points through the diffusion of Nb-containing phases, the growth of these phases could explain the accommodation of the strain seen in the tensile tests. If it is assumed that grain boundary sliding occurs along with grain rotation, which is reasonable since grains remain equiaxed after deformation, stress concentrations such as triple points and particles at grain boundaries can help to emit dislocations. Once emitted, the dislocations must move their way through the matrix to aid in accommodation of the resulting strain. In this case, it is possible for either grain boundary sliding, dislocation glide, or dislocation climb to be the rate-limiting step. With a strain rate sensitivity value of m=0.2, this rate limiting step should be the same as seen in power-law creep—the climb of dislocations within the grain interior and may be also responsible for the transition in deformation mechanism between 600 and 675 °C (Fig. 7). In some of the Fe-rich grains (Fig. 5b), there is some sort of particle-like diffraction contrast viewable in the center of the grains, which has not been identified yet, and may account for the obstacles that may be blocking the progress of dislocations, needed to justify the above proposed mechanism of deformation by dislocation climb-controlled creep.

5. CONCLUDING REMARKS

The current investigation has provided initial results of experimental research on deformation mechanisms in nanocrystalline material at elevated temperatures. In the absence of dislocation activity and grain growth (due to limited diffusivity) that was observed at 600 °C in the homogeneous nanocrystalline structure formed in Vitroperm alloy (Fig. 1a), only GB processes seem to be active during deformation. In this case, the material exhibits very high strain rate sensitivity. At the same time, low ductility suggests that these GB processes alone are

not able to support stable homogeneous deformation. Accommodation either by dislocation motion or by diffusion is needed to alleviate the extreme brittleness of NCM at low temperatures. The presence of isolated large grains ('large' meaning big enough for generation and/or motion of dislocations) in a nanocrystalline matrix has a beneficial effect on plastic behavior of NCM, while maintaining the high strength characteristics of the material. The crucial feature of this structure is isolation of large grains from each other within a finer-grained matrix. When these grains combine in groups, a dramatic drop in strength and ductility (but still higher than that for uniform nanostructure) was revealed. An important question that remains to be answered is: 'At what critical grain size do dislocations begin to take part in deformation?' The answer might be quite complicated because several factors seem to affect the dislocation motion in materials. For bcc materials this critical grain size might be larger than fcc in which, for example, a transition from unit dislocation to partials was detected by MDS and experimentally [9-11]. Such partials can be supported at very small grain sizes as compared with unit dislocations in bcc structures. Moreover, despite the fact that the homogenous nanocrystalline structure crystallized in Vitroperm alloy is single-phase, the presence of a large amount of alloying atoms in solid solution might strongly affect the intragrain dislocation motion. These alloying atoms might also function to pin GB thereby increasing thermal stability of nanostructures as seen in this work where an extremely fine structure is stable up to 600 °C.

The analysis of deformation mechanisms at extremely diminished length scale appears to be a very complicated task. The existence of multiple possible independent processes that might support the deformation flow, such as dislocation glide and climb, grain boundary migration, grain boundary sliding and grain rotation, new phase formation at triple points, twinning, shear banding, *etc.*, makes it difficult to isolate a particular controlling mechanism in NCM at particular conditions. It should be suggested that in most cases of deformation of NCM, a few independent processes are active simultaneously. For example, during deformation of initially homogeneous nanocrystalline Vitroperm at 725 °C (Fig. 6a), steady state flow seems to be supported by grain boundary sliding accommodated by grain boundary migration and formation of a new phase (or phases) at triple points. This flow occurs up to a point when the grains became large enough for extensive dislocation activity that leads to catastrophic necking and failure. In the material with an initially bimodal grain size distribution, a portion of grains are already large enough to provide dislocation motion and necking starts much earlier in this case (Fig. 6a, curve 2).

Further experiments are needed to fully determine the effects of structure on deformation mechanisms in NCM. Some of these experiments are in progress at present.

ACKNOWLEDGEMENTS

The authors would like to acknowledge the National Science Foundation, Division of Materials Research for its financial support under grant NSF-DMR-0240144 and Chris Nelson at the National Center for Electron Microscopy (NCEM) at Lawrence Berkeley laboratory (LBL). Proposal #257 fo electron microscopy support.

REFERENCES

[1] R.S. Mishra and A.K. Mukherjee, In: *Superplasticity and Superplastic Forming. Proceedings of a Conference held as part of the TMS Annual Meeting* (TMS, 1998) p.109.

[2] A.V. Sergueeva, V.V. Stolyarov, R.Z. Valiev and A.K. Mukherjee // *Scripta Mater.* **45** (2001) 747.

[3] H. Hahn and R.S. Averback // *J.Amer.Ceram. Soc.* **74** (1991) 2918.

[4] K. Taketani, A. Uoya, K. Ohtera, T. Uehara, K. Higashi, A. Inoue and T. Masumoto // *J. Mater. Sci.* **29** (1994) 6513.

[5] K. Higashi // *Mater. Sci.Eng. A* **166** (1993) 109

[6] T. G. Nieh and J. Wadsworth// *Scripta mater* **25** (1991) 955.

[7] L. Lu, M.L. Sui and K. Lu// *Acta Mater.* **49** (2002) 4127.

[8] T. Kulik// *J. Non-cryst. Solids* **287** (2001) 145.

[9] H. Van Swygenhoven// *Science* **296** (2002) 66.

[10] V. Yamakov, D. Wolf, S. R. Phillpot, A. K. Mukherjee and H. Gleiter// *Acta Mater.* **50** (2002) 5005.

[11] X. Z. Liao, Y. H. Zhao, Y. T. Zhu, R. Z. Valiev and D. V. Gunderov// *J. Appl. Phys.* **96** (2004) 636.